OPEN ACCESS

University of BRISTOL

Anderson, H. R., & McGeehan, J. P. (1994). Assessing the effect of DS-CDMA chip rate on RAKE branch statistics using a ray-tracing propagation model. In International Symposium on Personal, Indoor and Mobile Radio Communications (PIMRC) The Hague, Netherlands. (Vol. 1, pp. 33 - 37). Institute of Electrical and Electronics Engineers (IEEE). 10.1109/WNCMF.1994.530762

Link to published version (if available):
10.1109/WNCMF.1994.530762

Link to publication record in Explore Bristol Research
PDF-document

Assessing the Effect of DS-CDMA Chip Rate on RAKE Branch Statistics Using a Ray-Tracing Propagation Model

H. R. Anderson[1] and J.P. McGeehan
Centre for Communications Research
University of Bristol
Queen's Building, University Walk
Bristol BS8 1TR United Kingdom
Tel: 44 272 303272 FAX: 44 272 255265

Abstract - An important improvement in the performance of CDMA and other wideband digital communication systems can be achieved using a RAKE receiver architecture and diversity combining of its branches. This paper presents an analysis of RAKE branch statistics as a function of chipping or channel symbol transmission rate for urban microcells. A deterministic ray-tracing model is used to provide realistic, site-specific estimates of the time dispersion in the dynamic fading channel. The results of the analysis show that increased chipping rates produce increasingly Ricean fading distributions on the diversity branches along with increased power in the higher order diversity branches. Increased diversity branch power results in more effective diversity combining and improved signal-to-noise ratios of the combined branch signals.

1. Introduction

The increasing demand for personal communication channels for public use has given rise to a number of techniques to augment the capacity of existing cellular telephone systems. These techniques include sectorized cells, microcells, adaptive antennas and wideband modulation techniques such as TDMA and CDMA which purport to increase assigned cellular spectrum capacity by a factor of 5 to 20[1].

CDMA systems use spread spectrum techniques in which the channel symbol spectrum is much greater than the information data rate - typically 50 to 1000 times greater. By spreading the information signal over a bandwidth greater than the signal bandwidth, and using generally orthogonal codes for the spreading signal modulation, multiple users can share the same spectrum space without causing destructive interference to one another. CDMA systems also inherently provide frequency diversity.

In a normal urban microcell propagation environment, the signal received at any location will consist of a multitude of components arriving by different transmission paths. The resulting multipath signal consists of the sum of transmitted signal replicas which are dispersed in time and whose amplitudes and phases

vary according to the particular elements along each transmission path. Normally such multipath represents destructive interference to a digital signal since the dispersed received signal energy causes intersymbol interference (ISI) for subsequent symbols. However, as the transmitted symbol duration decreases (transmitted bandwidth spreads), the individual multipath components (or time clusters of energy from multipath) can be resolved in time by the receiver.

Since the components arrive by different paths, their fading characteristics should be un-correlated. The resolved, un-correlated signals can be combined using standard diversity combining techniques to yield a net signal which does not exhibit the same degree of fading as a signal without diversity. Exploiting multipath signals in this way using a RAKE receiver was discussed in [2] for general spread spectrum signals. It was discussed in [3] and [4] for of CDMA systems.

The objective of the research presented here was to explore the statistical nature of the diversity branch signals in a RAKE receiver as the chip rate is changed. Measured results based on a few analysis points are given in [4]. The approach in the present research is to use a ray-tracing propagation model rather than measurements to determine the time dispersive properties of the channel. This allows a greater number of study points to be conveniently analyzed so that the results are based on much broader statistical sampling. The ray-tracing model also provides insight into the underlying propagation circumstances (reflection, diffraction, scattering, etc.) which lead to particular time dispersion characteristics.

The results of this work show that as expected the energy in the diversity branches increases as chip rate increases. The nature of the signal envelope statistics on the branches also changes, becoming more Ricean as the chip rate increases. This is consistent with the work reported in [4],[5], and [6]. However, the increased Ricean nature of the branch signals occurs for other branches, not just the first. This increase in K factor with chipping rate is also a strong function of the propagation environment. Both results are being used in further ray-tracing research to model the BER performance a RAKE receiver can provide under a variety of channel conditions.

---

[1] Also president of EDX Engineering, Inc., Eugene, Oregon USA.

2. Ray-Tracing Propagation Model

A general model for the low-pass impulse response for an urban radio channel is:

$$h(t) = \sum_{n=1}^{N} A_n \delta(t - \tau_n) \exp(-j(\theta_n + \Delta\theta_n))$$ (1)

in which the impulse response $h(t)$ is the sum of a set of N impulses arriving at delay times τ_n with amplitudes A_n, phases θ_n, and phase displacements $\Delta\theta_n$. The phase displacements result from the motion of the receiver or other spatial change of the receiver location relative to the rest of the propagation environment which may itself including moving objects (reflections from cars and buses, etc.). For a mobile receiver the displacement term is given by $\Delta\theta_n = (2\pi vt / \lambda)\cos(\phi_n + \phi_v)$, where ϕ_n is the arrival angle of the nth impulse, v is the speed of motion, and ϕ_v is the direction of motion.

To use this model, it is necessary to identify the amplitudes, time delays, and absolute phase shifts of the N components of $h(t)$. The received components consist of the line-of-sight signal from the transmitter and a variety of signals reaching the receive antenna via reflecting surfaces, diffracting corners and scattering surfaces. By using ray-tracing techniques, the energy emitted from the source transmitting antenna is geometrically traced to determine those surfaces or corners which are illuminated. For the ray-tracing model used here, each illuminated surface is replace by an image transmitter or scattering source such that the radiation from the image represents (in amplitude, phase, and radiating directions) the energy reflected from the source. Similarly, an illuminated corner is replaced by an equivalent wedge diffraction source. With the first set of images and illuminated corners in place, each of them is then considered in turn by ray-tracing to determine the surfaces and corners they illuminate. This process is repeated for as many iterations as may be relevant to the problem at hand, or which are practical from a computational point of view. The ray interactions with the propagation environment are tracked for both HP and VP by taking into account the conductivity and permittivity of the walls and corners, and the angle of incidence for the interaction at each wall and corner.

Ray-tracing has become a widely used technique for analyzing propagation in outdoor microcells and indoor wireless LAN systems. The theoretical model used here is described in detail in [7]. Ray-tracing models along with comparisons to measurements can be found in [8] and [9].

A typical ray tracing study for a transmitter at point AA to a receiver at point R is shown in Figure 1 along with the resulting power delay profile.

A ray-tracing propagation model only provides the ray amplitudes and phases to a single precise point. At this point it may happen that the vector sum of the rays result in a null (fade) or peak in the received voltage
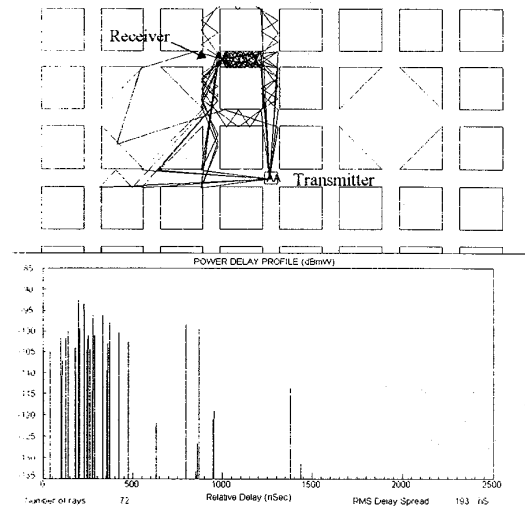

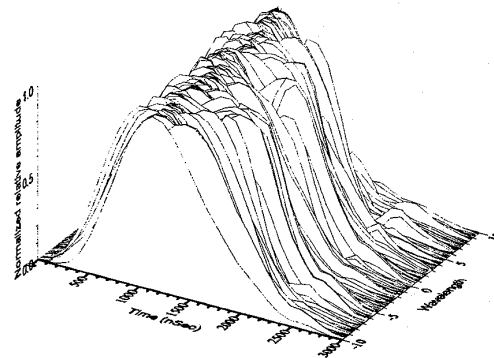Fig. 1. Ray-tracing study with power delay profile.

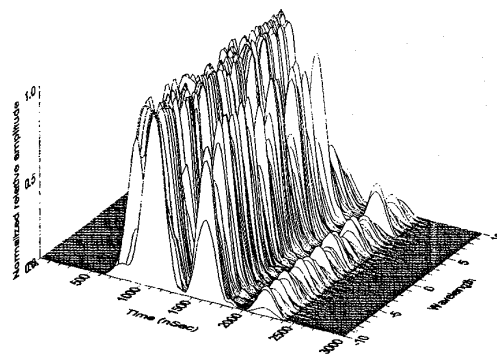Fig. 2. Time signatures with 1.25 MHz chipping rate.

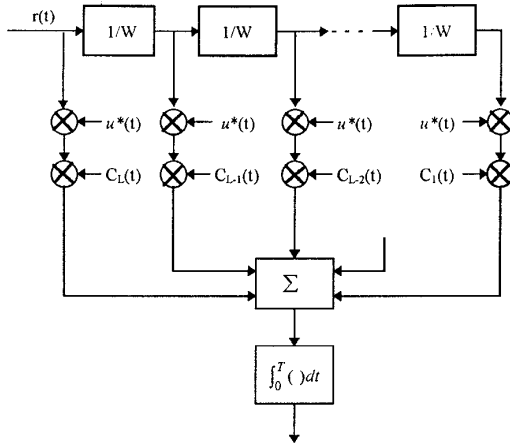Fig. 3. Time signatures with 5 MHz chipping rate.

Fig. 4. Basic RAKE receiver configuration.

envelope. However, in general the geometry of the environment is not known with sufficient accuracy to predict the envelope voltage precisely. For the carrier frequencies typically involved in PCS microcell systems (around 2000 MHz), the wavelength is on the order of 15 cm. In a typical urban building database, the building wall locations may only be known within perhaps one meter. Because absolute phase can't be known, it is necessary to determine the channel response over a range of positions around the precise location where the ray-tracing analysis was performed. This can be done by considering the *fading signature* over a range of wavelength displacements around this point. For a typical analysis, the fading signature is calculated at points every 0.125 wavelengths over a range of ±10 wavelengths in four crossing directions around the ray-tracing analysis point. This uniform pattern of four fade routes was used to reduce any anomalies which might result from the location of the point relative to the physical environment and the particular arrival angles of the rays.

3. Time Signature of Received Voltage with Fading

When a data symbol $u(t)$ is transmitted, the resulting received voltage $r(t)$ is the convolution of the data symbol voltage and the channel impulse response given by (1):

$$r(t) = \sum_{n=1}^{N} A_n\, u(t - \tau_n)\, \exp(-j(\theta_n + \theta_v)) + n(t) \qquad (2)$$

where $n(t)$ is the AWGN. For the studies done here, $u(t)$ was assumed to be the usual raised-cosine pulse:

$$u(t) = \frac{\sin(\pi t / T)}{\pi t / T}\, \frac{\cos(\beta \pi t / T)}{(1 - 4\beta^2 t^2 / T^2)} \qquad (3)$$

The pulse shape parameter β affects the spectral width and is generally set at 0.5 or 1.0 (actually 0.99 to avoid computational difficulties in (3)). A value of 1.0 was used for the studies reported here.

With a particular modulation type and data rate, the time signature of the channel for a given value of phase displacement or spatial displacement along a fade route can be found from (2). A sequence of such time signatures can be assembled by re-computing $r(t)$ at the set of incrementally-spaced positions along the fade routes described in Section 2. An example of such a sequence of time signatures over a ±10 wavelength fade route is shown in Figures 2 and 3. These time signatures were generated using BPSK modulation with data rates of 1.25 and 5 Mbps, respectively. The dynamic nature of the channel response over the fade route is clear.

4. RAKE Receiver Signal Branch Statistics

A simplified diagram of a RAKE receiver is shown in Figure 4 [10]. The received signal $r(t)$ is sent through a delay line with L-1 delays of $1/W$ = the time duration of the channel symbol. After each delay, the signal at the tap or branch is multiplied by the reference data signal pulse $u^*(t)$ and a coefficient $C_i(t)$ which depends on the amplitude of the channel energy in that branch. The L branch signals are summed and integrated over the symbol time spacing T to yield a decision variable. In this way the RAKE receiver is collecting the multipath energy resulting from the propagation environment and using it constructively.

Our specific interest here is in the statistics of the signal voltage at the output of each of the $1/W$ delays before it is multiplied by $u(t)$ and $C(t)$. To investigate these voltages, the time signatures like those shown in Figures 2 and 3 were created using the ray-tracing model. The complete time signature was then sampled 16 times every symbol period over several symbol periods to find the maximum value. This was established as the "0" branch. Around the exact point where the maximum was found, +8 other samples were computed and averaged. The result was a voltage value for the 0 branch for that particular point on the fade route. By establishing the branch with the maximum value, the analysis essentially tracks the peak through fading in a fashion analogous to that used in measurement analysis.

With the branch containing the peak determined, the voltage in adjacent branches -1 through 5 were found in the same way. This analysis was repeated at the next point along the fade route until all 640 points on the four crossing fade routes were considered. The statistics (mean and variance) of the 640 voltage values were then calculated.

Of particular interest here is the relative amplitudes of the mean voltages on the branches, and the Ricean K factor of the voltage distribution. If one presumes the

branch voltage pdf can be described by a Rice distribution of the form:

$$p(r) = \frac{r}{\sigma^2} \exp\left(\frac{-r^2}{2\sigma^2}\right) \exp\left(\frac{-A^2}{2\sigma^2}\right) I_o\left(\frac{rA}{\sigma^2}\right) \qquad (4)$$

where the K factor is then defined as:

$$K = 10\log_{10}\left(\frac{A^2}{2\sigma^2}\right) \qquad (5)$$

is a measure of the variability of the distribution around a constant amplitude component, A, which may be hypothetical. Although the Rice distribution is presumed to fit the actual values and may in fact not be a good fit in some cases, nevertheless it will serve our purpose here to compare the *relative* statistical nature of the voltages on the RAKE branches, especially as the chipping rate is increased (1/W is decreased).

If one assumes a Rice pdf, there is a one-to-one correspondence between the K factor and the ratio of the distribution mean $\bar{r}$ to the standard deviation, σ_r (note that this is not the same as σ in equations (4) and (5)). By calculating the ratio $\bar{r}/\sigma_r$ for several Rice pdf's with known values of K factor, a discrete function is developed. Working backwards, then, for any ratio $\bar{r}/\sigma_r$ from the branch voltage analysis the corresponding K factor can be determined.

For the mean voltage of the lth branch, the above described process can be written as:

$$\bar{v}_l = \frac{1}{N}\sum_{n=1}^{N}\frac{1}{T}\int_{-T/2}^{T/2} r_n(t + t_o + lT)\, dt \qquad (6)$$

where t_o is the sample time at the peak for each time signature n on the fade route. The variance is found in the usual way as the second central moment of the distribution.

5. RAKE Branch Statistics in an Urban Microcell Environment

The branch statistics as described in Section 4 were calculated at a set of points along the study route shown in Figure 5. This route includes 114 points spaced at 5 meter intervals, some of which are line-of-sight with the transmitter at point AA, and some of which are shadowed or in the "plaza" area where the RMS delay spread is higher due to the widely spaced opposing reflecting surfaces.

To get an overall view of branch statistics in this type of environment, the individual branch results for the 114 points were averaged. The route study was then repeated for values of T = 50, 100, 200, 400, and 800 nanoseconds, corresponding the chipping rates of 20, 10, 5, 2.5, and 1.25 MHz. The results for the K factor and
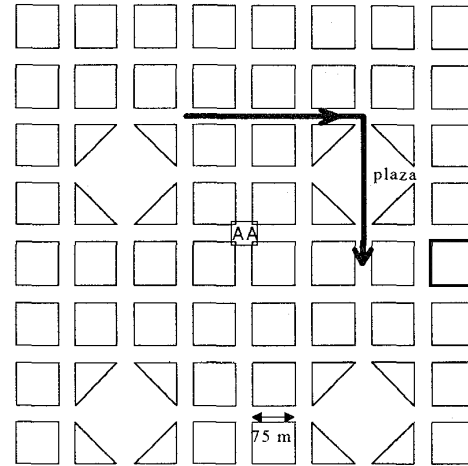

Fig. 5. Map of study route.

relative voltage levels on the branches as averaged over the fade routes are shown in Figures 6 and 7, respectively.

From Figure 6 it is clear that the K factor in the peak branch (0) increases with increasing chipping rate. The K factor in adjacent branches also increases. The increase in K factor in the peak branch 0 can in part be explained because the analysis tracked the peak, and as such, the voltage values on the branch represent a biased sampling of the time signatures. The same as not true for the first adjacent branches (-1 and +1). As the chipping rate increases, the number of rays arriving with in a given symbol period with decrease. It is plausible that this will increase the probability of a single ray dominating over the others arriving within that symbol period. With a dominate single ray, the K factor will increase. Note that the minimum value of K factor function described in Section 4. Such very negative values of K indicate an essentially Rayleigh pdf.

The results for the relative voltage levels in Figure 7 show that higher chipping rates lead to more power spread among the higher order RAKE branches. The relative difference in average levels in the peak branch (0 branch) was less than 1 dB across the five chipping rates tested, with the highest level at the lowest chipping rate of 1.25 MHz. It is somewhat surprising that the power difference in this branch is not greater than 1 dB since the 800 nSec branch window at 1.25 MHz will include may more rays than the 50 nSec window at the 20 MHz chipping rate. One possible explanation is that the branch power is still largely dominated by a few rays which constitute the main energy in the peak. The additional weaker rays included in the wider time window are relatively unimportant to the overall peak value.
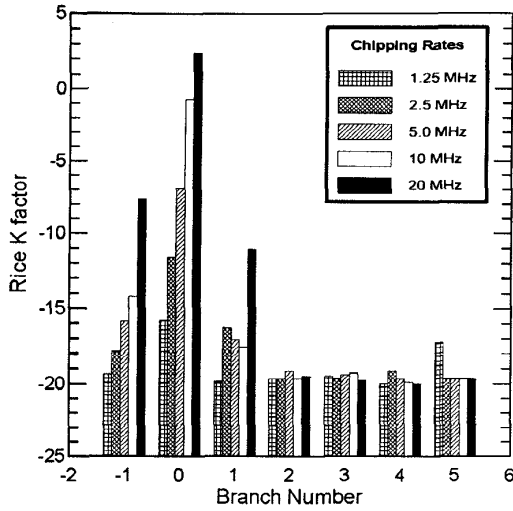
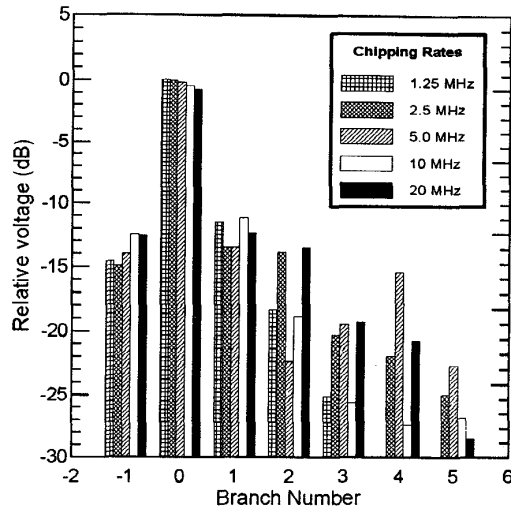**Fig. 6.** Rice K factors for voltages on RAKE diversity branches.

Fig. 7. Relative voltage amplitudes on RAKE diversity branches.

6. Conclusions

A method for investigating the statistics of the voltages on the branches of a RAKE receiver for different CDMA chipping rates has been presented. The approach uses a ray-tracing propagation model to provide realistic time signatures of the channel response through fading at a large number of study points along a route through a hypothetical urban environment. The time signatures directly provide the voltage responses at the RAKE branches.

The results show that as the chipping rate is increased the Rice K factor in the branch with the maximum voltage also increases. A less pronounced increase in K factor with chipping rate on the first adjacent branches also occurs.

This research also showed that the voltage distribution on the branches changes as the chipping rate increases with a broader distribution of energy across more branches as the chipping rate increases. The amount of power in the peak branch remained relatively unchanged as the chipping rate increased, with a minor though consistent decrease of about 1 dB as the chipping rate increased from 1.25 to 20 MHz.

It should be emphasized that these results are for a dense urban environment such as Manhattan which can be roughly characterized as having "urban canyons." While such propagation environments may be the most challenging to serve for microcell systems, they are not generally indicative of the majority of service area propagation environments which will be encountered by PCS system designers. Further research such as that presented here is continuing for a variety of typical sparsely urban and residential propagation environments.

7. Acknowledgment

8. References

[1] K.S. Gilhosen, I.M. Jacobs, R. Padovani, and A.J. Viterbi, "On Capacity of a Cellular CDMA System," *IEEE Trans. on Veh. Technol.*, vol. 40, pp. 303-312, May, 1991.

[2] G.L. Turin, "Introduction to spread-spectrum antimultipath techniques and their application to urban digital radio," *Proc. of the IEEE*, vol. 68, No. 3, March 1980, pp. 328-353.

[3] M.A. Beach, A. Hammer, S.A. Allpress, J.P. McGeehan, and A. Bateman, "An Evaluation of Direct Sequence CDMA for Future Mobile Personal Communication Networks," *Proceedings of the 41st IEEE Veh. Tech. Conference*, St. Louis, pp. 63-70, May 1991.

[4] S.A. Allpress et. al., "An Investigation of RAKE Receiver Operation in an Urban Environment for Various Spreading Bandwidth Allocations," *Proc. of the 41st IEEE Veh. Tech. Conf.*, Denver, pp. 506-510, May 1992.

[5] S.A. Allpress, M.A. Beach and J.P. McGeehan, "On the optimum DS-CDMA channel bandwidth for personal communication systems," *Proc. of the 42nd IEEE Veh. Tech. Conf.*, Secaucus, pp. 436-439, May 1993.

[6] M.A. Beach and S.A. Allpress, "Propagation aspects of mobile spread spectrum networks", Chapter 12 in *Radiowave Propagation*, Editors M.P.M Hall, L.W. Barclay and M.T Hewitt. Peter Peregrinus Limited. (To be published).

[7] H.R. Anderson, "A ray-tracing propagation model for digital broadcast systems in urban areas," *IEEE Trans. on Broadcasting*, Vol. 39, no. 3, Sept. 1993, pp. 309-317.

[8] K.S. Schaubach, N.J. Davis and T.S. Rappaport, "A ray-tracing method for predicting path loss and delay spread in microcell environments," *Proceedings of the 1992 Veh. Tech. Society Conf.*, Denver, pp. 932-935, May 1992.

[9] M.C. Lawton and J.P. McGeehan, "The application of GTD and ray launching techniques to channel modelling for cordless radio systems," *Proc. of the 41st IEEE Veh. Tech. Conf.*, Denver, pp. 125-130, May 1992.

[10] J. Proakis. *Digital Communications*. New York: McGraw-Hill, 1989, p. 732.